Fluorescent Chemosensors for Divalent Zinc Based on Zinc Finger Domains. Enhanced Oxidative Stability, Metal Binding Affinity, and Structural and Functional Characterization

Grant K. Walkup and Barbara Imperiali*

Contribution from the Division of Chemistry and Chemical Engineering, California Institute of Technology, Pasadena, California 91125

Received December 6, 1996[⊗]

Abstract: The design, synthesis, and characterization of a family of peptides modeled after the zinc finger domains, which has led to the production of a fluorescent peptidyl sensor for divalent zinc with enhanced oxidative stability, are reported. The chemosensor design comprises a synthetic peptidyl template and a covalently attached fluorescent reporter which is sensitive to metal-induced conformational changes in the polypeptide construct. The modular synthetic approach employed for the construction of these chemosensors allows independent modification of the metal coordination sphere and the fluorescent reporter group. The structural, fluorescence, and zinc binding properties of these peptides and the effects of integrating various environment sensitive fluorophores, 4-(dimethylamino)-benzamide, 5-(dimethylamino)naphthalenesulfonamide, and 3-carboxamidocoumarin, are described. Manipulation of the ligand sphere, by removal of one of the pair of thiolate ligands, was undertaken to enhance the oxidative stability of the chemosensor. For each of these peptides, the apparent dissociation constant of the peptide−zinc complex has been determined by spectroscopic methods. High-affinity binding, with dissociation constants ranging from 7 pM to 65 nM, is observed.

Introduction

Fluorescent indicators have revolutionized the process of quantifying metal cations in aqueous media, and in particular within biological samples. The importance of fluorescent indicators for the intracellular measurement of sodium and potassium,[1] calcium,[2,3] magnesium,[4] and pH[5,6] is well known. Due to the success of these agents, the design and production of fluorescent chemosensors for other species continues to be an active area of interest.

The central problem in the production of new fluorescent sensors for the detection of metal cations lies in selectivity.[7] In fact, there are successful intracellular fluorescent probes only for the divalent cations Mg^{2+} and Ca^{2+}, which are present at the highest concentration within the cell. For example, the concentration of ionized Zn^{2+} within a cell or in sea water is commonly 10^6-fold less than that of Mg^{2+} or Ca^{2+}.[8,9] Thus, the fluorescent indicator fura-2 may bind Zn^{2+} with greater affinity than Ca^{2+}, but remains a cellular probe for free calcium. In order to prevent spurious cross-talk, the relative affinity of the sensor for the ion of interest must exceed the cumulative concentration excess imposed by all other competing species.

Typically, this difficulty has been addressed by the exploitation of proteins for their unmatched selectivity in binding small molecules.[10] Thus, biological signal transducers, i.e., "biosensors", have been devised from existing proteins for the divalent cations of zinc,[11,12] mercury,[13] copper and cobalt,[14] and even organic molecules such as cAMP.[15]

The need for new chemosensors for many analytes continues to exist.[16] Although the analyte binding selectivity which may be obtained with a biosensor is remarkable, the complexity of a large biomolecule can impose greater design constraints relative to an abiotic sensing molecule. For example, proteins typically lack the fluorescence characteristics of a useful sensor, and thus a strategy involving affinity labeling or an auxiliary diffusible fluorophore is required for signal transduction. In this light, the production of a purely synthetic chemosensor is desirable as there is greater flexibility for systematic variation of the analyte binding and fluorescent moieties of the sensor. The recent production of peptidyl motifs with tunable metal binding properties,[17] as well as those with novel fluorescent signaling capabilities,[18] highlights the applicability of this technique.

We have investigated the production of zinc-responsive fluorosensors using a hybrid approach. By exploiting the selective metal binding properties of the zinc finger domains,[19]

⊗ Abstract published in *Advance ACS Abstracts,* April 1, 1997.
(1) Minta, A.; Tsien, R. Y. *J. Biol. Chem.* **1989,** *264,* 19449−19457.
(2) Tsien, R. Y. *Biochemistry* **1980,** *19,* 2396−2404.
(3) Grynkiewicz, G.; Poenie, M.; Tsien, R. Y. *J. Biol. Chem.* **1985,** *260,* 3440−3450.
(4) Raju, B.; Murphy, E.; Levy, L. A.; Hall, R. D.; London, R. E. *Am. J. Physiol.* **1989,** *256,* C540−C548.
(5) Bassnett, S.; Reinisch, L.; Beebe, D. C. *Am. J. Physiol.* **1990,** *258,* C171−C178.
(6) Rink, T. J.; Tsien, R. Y.; Pozzan, T. *J. Cell Biol.* **1982,** *95,* 189−196.
(7) Czarnik, A. W. Supramolecular Chemistry, Fluorescence, and Sensing. In *Fluorescent Chemosensors for Ion and Molecule Recognition*; Czarnik, A. W.; Ed.; ACS: Washington DC, 1993; pp 1−9.
(8) Bruland, K. W. In *Trace Elements in Sea Water*; Rilet, J. P., Chester, R., Eds.; Academic Press: London, 1975; pp 157−220.
(9) Fraústo da Silva, J. J. R.; Willams, R. J. P. *The Biological Chemistry of the Elements: The Inorganic Chemistry of Life*; Clarendon Press: New York, 1993.

(10) Giuliano, K. A.; Post, P. L.; Hahn, K. M.; Taylor, D. L. *Annu. Rev. Biophys. Biomol. Struct.* **1995,** *24,* 405−434.
(11) Thompson, R. B.; Jones, E. R. *Anal. Chem.* **1993,** *65,* 730−734.
(12) Thompson, R. B.; Patchan, M. W. *Anal. Biochem.* **1995,** *227,* 123−128.
(13) Virta, M.; Lampinen, J.; Karp, M. *Anal. Chem.* **1995,** *67,* 667−669.
(14) Thompson, R. B.; Ge, Z.; Patchan, M.; Huang, C.-C.; Fierke, C. A. *Biosens. Bioelectron.* **1996,** *11,* 557−564.
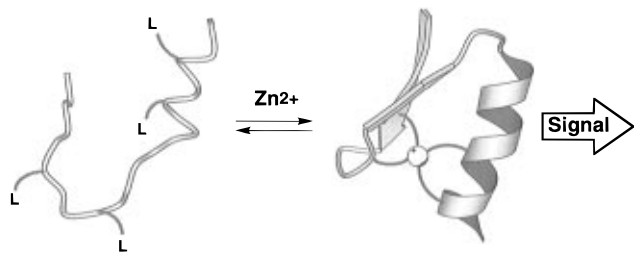(15) Adams, S. R.; Harootunian, A. T.; Buechler, Y. J.; Taylor, S. S.; Tsien, R. Y. *Nature* **1991,** 694−697.
(16) Czarnik, A. W. *Chem. Biol.* **1995,** *2,* 423−428.
(17) Cheng, R. P.; Fisher, S. L.; Imperiali, B. *J. Am. Chem. Soc.* **1996,** *118,* 11349−11356.
(18) Torrado, A.; Imperiali, B. *J. Org. Chem.* **1996,** *61,* 8940−8948.

Scheme 1

we have sought to combine the advantageous aspects of both abiotic chemosensors and biosensors within a synthetic polypeptide architecture. Zinc finger peptides bind divalent zinc avidly, with dissociation constants as low as 5.7 pM reported for the peptide·Zn^{2+} complex,[20] and with great selectivity.[20,21] A single zinc finger domain is 25−30 residues in length and may be described by the consensus sequence (F/Y)-X-C-X_{2-4}-C-X_3-F-X_5-L-X_2-H-X_{3-5}-H-X_{2-6}.[22,23] Importantly, peptides of these lengths are synthetically accessible by chemical techniques. Furthermore, zinc fingers have been shown to undergo reversible metal-induced folding,[24,25] which nucleates a cluster of hydrophobic residues (underlined above).

Recently we reported the synthesis and characterization of a fluorescent peptidyl chemosensor for divalent zinc, patterned after the zinc fingers.[26] An aromatic residue of the hydrophobic cluster of the parent sequence was replaced with a derivative of β-aminoalanine, incorporating an orthogonally protected side-chain amine. At the completion of the peptide synthesis, this residue may be selectively deprotected and then coupled with a variety of amine-reactive fluorophores to produce a selectively labeled fluorescent peptide. Deprotection and cleavage of the peptide from the synthesis resin affords the completed chemosensor. The microenvironment experienced by the fluorophore-bearing residue changes upon peptide·Zn^{2+} complex formation, resulting in enhanced fluorescence. A depiction of this mechanism for signal transduction is shown in Scheme 1.[27] In addition, we note the subsequent report of another sensor developed along similar lines,[28] but which uses two fluorophores and a resonant energy transfer mechanism for signal transduction.

Both of these sensors are capable of quantifying nanomolar concentrations of Zn^{2+}, but are susceptible to oxidation through the formation of an intramolecular disulfide bond and are thus incompatible with aqueous oxidants including oxygen and redox active ions such as Cu^{2+}. This may not be problematic in the reducing environment of a cell, but application of these sensors toward the measurement of environmental samples would be precluded.

Herein we report the design, synthesis, and characterization of the family of zinc finger peptides, which has led to the production of a fluorescent peptidyl sensor for divalent zinc

Table 1. Amino Acid Sequences of the Synthetic Zinc Finger Peptides

peptide	sequence[a]
FS01DMB	Ac-B(DMB)ACDICGKNFSQSDELTTHIRTHT-NH_2
FS02DNS	Ac-B(DNS)ACDIHGKNFSQSDELTTHIRTHT-NH_2
FS02CMN	Ac-B(CMN)ACDIHGKNFSQSDELTTHIRTHT-NH_2
FS03DNS	Ac-YQCQYCEKRB(DNS)ADSSNLKTHIKTKHS-NH_2
FS04DNS	Ac-YQCQYDEKRB(DNS)ADSSNLKTHIKTKHS-NH_2

[a] The standard one-letter convention for naming amino acids has been followed. The residue "B" refers to (S)-2,3-diaminopropionic acid or L-β-amino alanine (Baa). The three letters in parentheses following this residue denote the covalently attached chromophore: DMB = 4-(dimethylamino)benzamide, DNS = 5-(dimethylamino)naphthylene-sulfonamide (dansyl), CMN = 3-carboxamido coumarin, DNC = 5-(dimethylamino)naphthalene-1-carboxamide.

Table 2. Apparent Dissociation Constants for Peptide·Zn^{2+} Complexes

peptide	coordination sphere	K'_D	peptide	coordination sphere	K'_D
FS01DMB	Cys_2His_2	7 pM[a]	FS03DNS	Cys_2His_2	140 pM[c]
FS02DNS	$CysHis_3$	3 nM[b]	FS04DNS	$CysAspHis_2$	65 nM[b,d]

[a] Determined by competitive titration with Co^{2+} and Zn^{2+}. [b] Determined by competition with the indicator mag-fura-2 for Zn^{2+}. [c] Determined by competition with the indicator 4-(2-pyridylazo)resorcinol for Zn^{2+}. [d] Initially forms a presumed 2:1 peptide−metal complex at low concentrations (≤20 nM) of free Zn^{2+}. The value represents the apparent value at ≥20 nM free Zn^{2+}.

with enhanced oxidative stability. The structural, fluorescence, and zinc binding properties of these peptides are described.

Results

Modular Fluorophore Incorporation. A key feature in the synthesis of these peptides is the residue (S)-2,3-diamino-N^α-(9-fluorenylmethyloxycarbonyl)-N^β-(allyloxycarbonyl)propanoic acid (Fmoc-L-Baa(alloc)-OH).[29] This residue may be incorporated at any position within the polypeptide chain. At the completion of synthesis but prior to peptide cleavage, the side chain may be selectively deprotected under mild conditions using a palladium catalyst.[30] The liberated amine is then available for coupling with a variety of fluorophores. The modularity of peptide synthesis is preserved through this strategy for fluorophore introduction.

The sequences of the peptides discussed in this paper are shown in Table 1. The amino acid sequence of each "fluorescent sensor" peptide has been denoted with the first four letters of its name (i.e., FS01, FS02, etc.), with the last three letters representing the fluorophore incorporated (see below). In addition, the previously reported fluorescent sensing peptide (ZNS1) will be referred to as FS03DNS, consistent with the terminology used for the remainder of the peptides discussed in this text. The standard one-letter convention for naming amino acids has been adopted with the addition of the nonstandard amino acid β-aminoalanine, which is represented by the letter B. The three letters in parentheses following this residue denote which chromophore is covalently attached to the side-chain amine of this residue. The abbreviations used, and the structures they represent, are DMB = 4-(dimethylamino)-benzamide, DNS = 5-(dimethylamino)naphthalenesulfonamide (dansyl), and CMN = 3-carboxamido coumarin. The structures and a summary of some of the fluorescence properties of these molecules[31] are shown in Figure 1.

(19) Berg, J. M.; Merkle, D. L. *J. Am. Chem. Soc.* **1989**, *111,* 3759−3761.

(20) Krizek, B. A.; Merkle, D. L.; Berg, J. M. *Inorg. Chem.* **1993**, *32,* 937−940.

(21) Krizek, B. A.; Berg, J. M. *Inorg. Chem.* **1992**, *31,* 2984−2986.

(22) Berg, J. M. *Acc. Chem. Res.* **1995**, *28,* 14−19.

(23) Klug, A.; Schwabe, J. W. R. *FASEB J.* **1995**, *9,* 597−604.

(24) Eis, P. S.; Lakowicz, J. R. *Biochemistry* **1993**, *32,* 7981−7993.

(25) Frankel, A. D.; Berg, J. M.; Pabo, C. O. *Proc. Natl. Acad. Sci. U.S.A.* **1987**, *84,* 4841−4845.

(26) Walkup, G. K.; Imperiali, B. *J. Am. Chem. Soc.* **1996**, *118,* 3053−3054.

(27) Kraulis, P. J. *J. Appl. Crystallogr.* **1991**, *24,* 946−950.

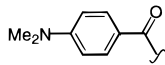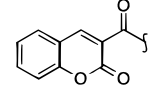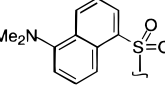(28) Godwin, H. A.; Berg, J. M. *J. Am. Chem. Soc.* **1996**, *118,* 6514−6515.

(29) Sinha Roy, R. Ph.D. Thesis, California Institute of Technology, 1996.

(30) Kates, S. A.; Daniels, S. B.; Albericio, F. *Anal. Biochem.* **1993**, *212,* 303−310.

(31) Haughland, R. P. Covalent Fluorescent Probes. In *Excited States of Biopolymers*; Steiner, R. F., Ed.; Plenum: New York, 1983; pp 29−58.

	λ_{ex} nm	λ_{em} nm	Q
Me₂N—C₆H₄—C(O)— **DMB**	310	475 - 525	0 - 0.1
CMN	315	400 - 450	0.05 - 0.3
DNS	335	500 - 550	0.05 - 0.5

Figure 1. Structures of some fluorophores incorporated within zinc finger peptides and their spectral properties. *Q* is the solvent-dependent quantum yield (values were taken from the literature[31]).
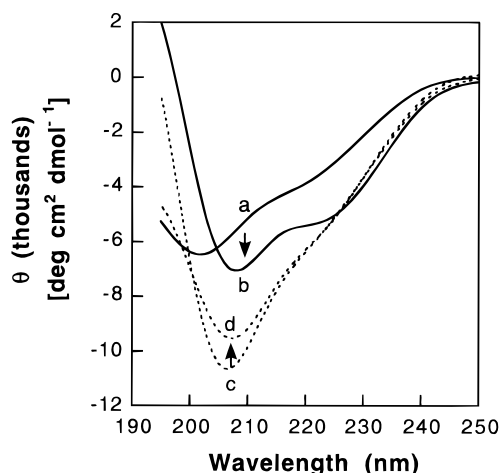

Figure 2. Circular dichroism spectra of FS01DMB (solid lines) and FS02DNS (dotted lines) in 0.5 mM HEPES, pH 7.0, in both the absence and presence of divalent zinc: (a) 12.9 μM FS01DMB; (b) 12.9 μM FS01DMB, 14 μM ZnCl₂; (c) 9.2 μM FS02DNS; (d) 9.2 μM FS02DNS, 14 μM ZnCl₂.

FS01DMB. The initial design of a fluorescent zinc finger peptide was based upon the sequence and structural information available from a crystal structure of Zif268.[32] The microenvironment sensitive fluorophore DMB was chosen for its unique spectroscopic properties. Unlike most solvent sensitive fluorophores, this molecule responds to decreasing microenvironment polarity with the production of a significantly red-shifted emission.[33] A chemosensor that exploits this property of DMB chromophore for polarity-dependent signaling has been previously reported.[34] The fluorophore was attached to the peptide as the *N*-terminal residue of the hydrophobic cluster. Unfortunately, the fluorescence emission of this peptide was insensitive to the addition of divalent zinc.

Circular dichroism (CD) studies were undertaken to probe whether metal-dependent structural changes could be observed. The CD spectra of FS01DMB at pH 7.0, alone and in the presence of an excess of Zn²⁺, are shown in Figure 2. The structural changes which accompany zinc addition are similar to those seen for other zinc finger peptides.[25,35,36] Additionally,

(32) Pavletich, N. P.; Pabo, C. O. *Science* **1991**, *252*, 809−817.

(33) Bhattacharyya, K.; Chowdhury, M. *Chem. Rev.* **1993**, *93*, 507−535.

(34) Hamasaki, K.; Ikeda, H.; Nakamura, A.; Ueno, A.; Toda, F.; Suzuki, I.; Osa, T. *J. Am. Chem. Soc.* **1993**, *115*, 5035−5040.

(35) Párraga, G.; Horvath, S. J.; Eisen, A.; Taylor, W. E.; Hood, L. E.; Young, E. T.; Klevit, R. E. *Science* **1988**, *241*, 1489−1492.

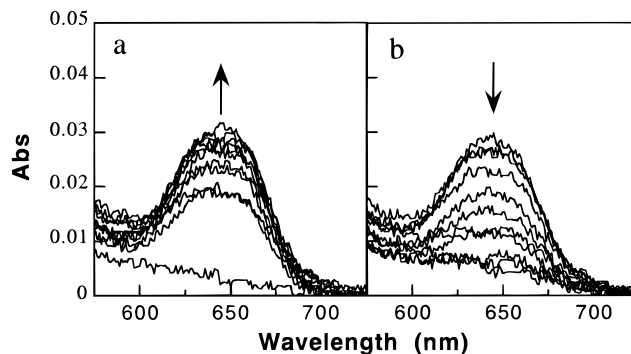(36) Weiss, M. A.; Mason, K. A.; Dahl, C. E.; Keutmann, H. T. *Biochemistry* **1990**, *29*, 5660−5664.

Figure 3. (a) Absorption spectra of 3.3 μM FS01DMB (path length 10 cm) upon addition of CoCl₂ up to 100 μM in 10 mM HEPES, pH 7.0. (b) Absorption spectra of the same upon the subsequent addition of ZnCl₂ up to 8.5 μM.

the Zn²⁺-induced change in the CD spectra is pH dependent, with no structural change apparent at pH ≤ 4. Again, this is similar to that for a zinc finger peptide characterized previously.[37]

The metal binding affinity of this peptide was probed by UV−vis spectroscopy to verify that the peptidyl template would bind Zn²⁺ with the avidity characteristic of the zinc finger domains and test whether the incorporation of the fluorescent probe significantly interferes with zinc binding. Because Zn²⁺ is a spectroscopically silent ion with an electronic configuration of d¹⁰, the determination of the Zn²⁺ binding affinity of zinc fingers has commonly been determined through competition experiments with Co²⁺.[19,38] Within the tetrahedral S₂N₂ coordination geometry of a zinc finger a d−d transition of bound Co²⁺ is observed.[39] This technique was used to probe the Zn²⁺ binding properties of FS01DMB. The metal cation titration of FS01DMB was monitored by UV−vis spectroscopy as illustrated in Figure 3. The dissociation constants for both the Co²⁺- and Zn²⁺-bound species were obtained from calculations using the absorption data obtained at 645 nm.

Mathematical treatment of the data was based on a simple two-state equilibrium described by the Scott equation.[40] Dissociation constants were obtained from an iterative calculation procedure in which successive approximations of $[M^{2+}]_{free}/b\Delta A$ (ordinate) are plotted against $[M^{2+}]_{free}$ (abscissa), where $[M^{2+}]_{free}$ is the free divalent metal in solution, *b* is the path length of the cell, and ΔA is the absorbance change observed. For initial calculations, only the higher metal concentrations were plotted in the assumption that $[M^{2+}]_{total} \approx [M^{2+}]_{free}$. By doing so, $[M^{2+}]_{free}$ values were estimated more accurately, and the procedure repeated until convergence occurred. From the final plot, the apparent dissociation constant is obtained from the *y*-intercept/slope. In the case of the Zn²⁺ titration, a relative dissociation constant was determined, which was multiplied by the Co²⁺ complex K_d to give the apparent peptide·Zn²⁺ complex K_d. Representative plots showing the final iteration of calculations for both Co²⁺ addition and Zn²⁺ competition are shown in Figure 4. The dissociation constants obtained were 2.8 μM for the Co²⁺ complex and 7 pM for the Zn²⁺ complex.

FS02CMN and FS02DNS. The polarity dependence of long-wavelength emission for the DMB chromophore stimulated the initial interest in this group as a fluorescent reporter. However, with the undesirable emission properties of FS01DMB, other

(37) Krizek, B. A.; Amann, B. T.; Kilfoil, V. J.; Merkle, D. L.; Berg, J. M. *J. Am. Chem. Soc.* **1991**, *113*, 4518−4523.

(38) Maret, W.; Vallee, B. L. *Methods Enzymol.* **1993**, *226*, 52−71.

(39) Bertini, I.; Luchinat, C. *Adv. Inorg. Biochem.* **1984**, *6*, 71−111.

(40) Connors, K. A. *Binding Constants: The Measurement of Molecular Complex Stability*; Wiley-Interscience: New York, 1987; p 411.
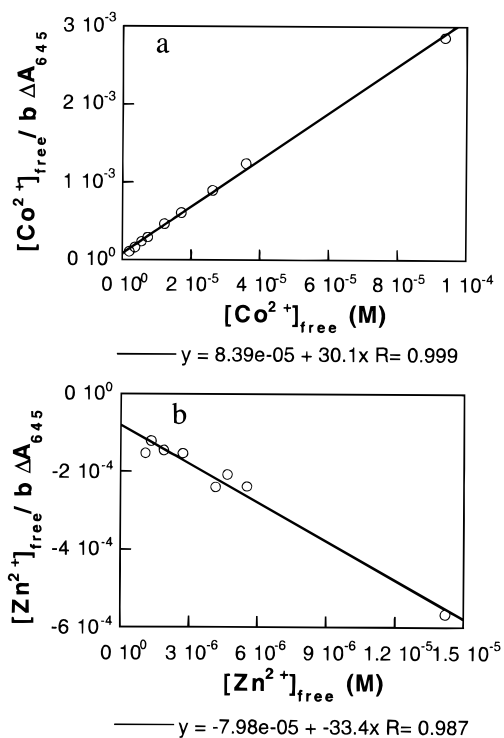
Figure 4. Analysis of the data obtained from Figure 3 where 3.3 μM FS01DMB is titrated with CoCl$_2$ up to 100 μM followed by titration with ZnCl$_2$ up to 8.5 μM. The ratio of *y*-intercept/slope gives the apparent dissociation constant of (a) 2.8 μM for the Co^{2+} complex and (b) 7 pM for the Zn^{2+} complex.

fluorophores were investigated for the next generation peptide. Fluorophores were chosen to be small in size in order to be well accommodated within the hydrophobic cluster, yet with known polarity-dependent emission properties. As a result, the fluorophores CMN and DNS were chosen for incorporation within the FS02 template. In addition, the substitution Cys^6 → His was made to probe the effect of changing the metal coordination sphere to one incapable of forming an intramolecular disulfide. This peptide provided the initial access to an oxidatively stable peptidyl template.

The effect of Zn^{2+} on the fluorescence emission of FS02DNS and FS02CMN was investigated. The dansylated peptide FS02DNS showed metal-induced fluorescence changes, whereas FS02CMN did not. As a consequence only FS02DNS was investigated further. The effects of zinc addition on the fluorescence of FS02DNS are summarized in Table 3.

To assess the structural implications of ligand replacement within the zinc finger motif, CD spectra were obtained and the zinc binding affinity of FS02DNS was investigated. The Zn^{2+}-induced structural changes of the CysHis$_3$ motif are minimal, which is consistent with the small increase in fluorescence intensity.

Addition of Co^{2+} to FS02DNS did not produce a d−d absorption band indicative of tetrahedral coordination. Thus, the zinc binding affinity of FS02DNS was assayed by a competition experiment with furaptra (mag-fura-2).[4] Mag-fura-2 forms a 1:1 complex with Zn^{2+}, with a dissociation constant of 20 nM determined via fluorescence measurements.[41] However, large shifts in the UV−vis absorption spectrum are observed upon the addition of Zn^{2+} as well. Consequently the competition was monitored by absorption spectroscopy, to avoid interference from the fluorescence of the peptide itself. In the absence of divalent zinc, the absorbance maximum of mag-

(41) Simons, T. J. B. *J. Biochem. Biophys. Methods* **1993**, *27*, 25−37.

Table 3. Fluorescence Emission Properties of Peptide·Zn^{2+} Complexes[a]

peptide	$\lambda_{\mathrm{max}}^{\circ}$ [c]	$\lambda_{\mathrm{max}}^{\mathrm{Zn}}$ [d]	$F_{\lambda\mathrm{max}}^{\mathrm{Zn}}$ [e]	$FE_{\lambda\mathrm{max}}$ [f]
FS02DNS	552	548	1.3	1.3
FS03DNS	560	525	2.4	3.0
FS04DNS	560	543	1.7	1.8
DNS-Asn[b]	560	560		

[a] Data were acquired with excitation at 333 nm in 50 mM HEPES, pH 7.0, 0.5 M NaCl. Data for FS03DNS were acquired with the addition of 50 mM MgCl$_2$, and 10 mM CaCl$_2$, 100 μM CoCl$_2$. Data for FS04DNS were acquired with the addition of 50 mM MgCl$_2$, 10 mM CaCl$_2$, and 0.1 μM each FeCl$_2$, CoCl$_2$, NiCl$_2$, CuCl$_2$, and CdCl$_2$. [b] Dansyl asparagine. [c] Wavelength of maximum emission for the peptide in the absence of divalent zinc. [d] Wavelength of maximum emission for the peptide·Zn^{2+} complex. [e] Fluorescence intensity of the peptide·Zn^{2+} complex at $\lambda_{\mathrm{max}}^{\mathrm{Zn}}$ normalized such that the fluorescence intensity at $\lambda_{\mathrm{max}}^{\circ} = 1$. [f] The fluorescence enhancement at the wavelength $\lambda_{\mathrm{max}}^{\mathrm{Zn}}$; defined as $FE_{\lambda\mathrm{max}} \equiv F_{\lambda\mathrm{max}}^{\mathrm{Zn}}/I$ where I is the fluorescence intensity at $\lambda_{\mathrm{max}}^{\mathrm{Zn}}$ in the absence of divalent zinc.
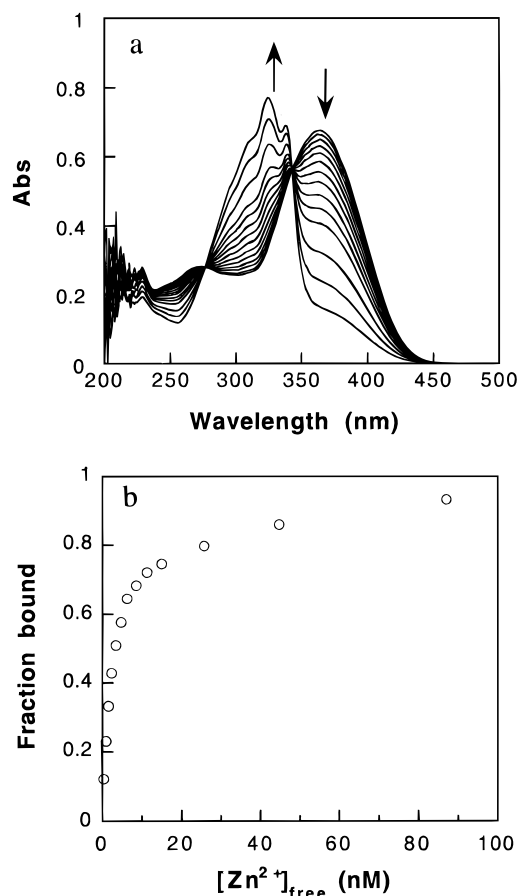

Figure 5. (a) Absorbance spectra of 13.0 μM FS02DNS and 22.6 μM mag-fura-2 upon addition of ZnCl$_2$ up to 32 μM in 50 mM HEPES, pH 7.0, $\mu = 0.15$ (NaCl). (b) Binding isotherm calculated from the data in (a).

fura-2 occurs at 366 nm, with an extinction coefficient of 29 900 M^{-1} cm^{-1}. When mag-fura-2 is bound to Zn^{2+}, the absorbance maximum blue-shifts to 325 nm, and the extinction coefficient at 366 nm decreases to 1880 M^{-1} cm^{-1}. A typical titration in which aliquots of ZnCl$_2$ are added to a solution of FS02DNS and mag-fura-2, and the corresponding binding isotherm for the formation of peptide·Zn^{2+} complex are shown in Figure 5. The dissociation constant calculated for the FS02DNS·Zn^{2+} complex was 3.0 ± 0.5 nM.

FS03DNS. The results from the first two generations of fluorescent sensing peptides indicated that judicious placement of the fluorophore is required for the generation of a significant
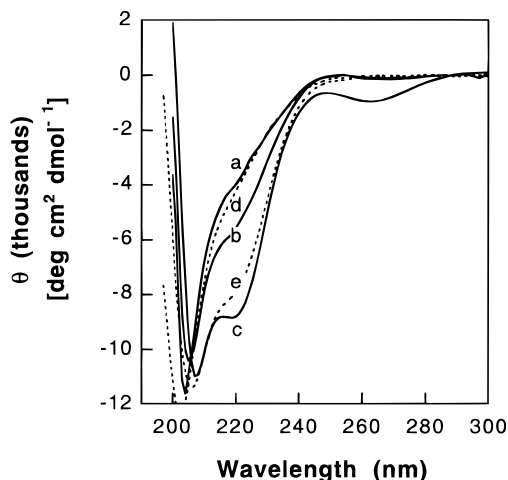
Figure 6. Circular dichroism spectra of FS03DNS (solid lines) and FS04DNS (dotted lines) in 0.5 mM HEPES, pH 7.0: (a) 9.6 μM FS03DNS; (b)12.3 μM FS03DNS, 120 μM CoCl$_2$; (c) 12.2 μM FS03DNS, 14.5 μM ZnCl$_2$; (d) 8.6 μM FS04DNS; (e) 8.6 μM FS04DNS, 10 μM ZnCl$_2$.

Figure 7. Absorption spectra of 240 μM PAR, in 50 mM HEPES, pH 7.0, upon the addition of (a) 10.6 μM ZnCl$_2$, (b) 3.49 μM FS03DNS, (c) 6.96 μM FS03DNS, (d) 10.4 μM FS03DNS, (e) 17.3 μM FS03DNS, (f) 27.5 μM FS03DNS.

change in fluorescence upon metal binding. In addition the peptidyl template must be able to tolerate the inclusion of the chromophore within the hydrophobic cluster. We examined the published solution structures of several zinc fingers,[42–45] with particular attention given to work in which residues which comprise the hydrophobic cluster were varied. As a result, the zinc finger domain "ZFY-swap"[46] was selected as the template, with Phe[10] of that sequence chosen for replacement with the dansylated Baa amino acid derivative, as opposed to position 1 which was used for the first two generation peptides.

The fluorescence properties and zinc sensing behavior of FS03DNS, which are sensitive to nanomolar concentrations of divalent zinc, have been reported previously.[26] The circular dichroism and zinc binding affinity of this peptide are now presented. The structural response of FS03DNS to different divalent metal cations is markedly different (Figure 6, solid lines). In the absence of divalent metal cations, the CD spectrum of FS03DNS appears to be predominantly random coil, similar to other zinc finger domains, and the FS03DNS·Zn^{2+} species has a CD spectrum that is characteristic of natural Zn^{2+}-bound zinc finger domains. By comparison, the FS03DNS·Co^{2+} species has a CD spectrum which is much less negative at 222 nm than that of the FS03DNS·Zn^{2+} complex, suggesting that less helical content is present in the Co^{2+} complex.

Similar to FS02DNS, the Co^{2+} complex of FS03DNS did not display a diagnostic d–d absorption band between 600 and 700 nm. However, the zinc binding affinity of FS03DNS is too high to be assayed accurately with mag-fura-2. An alternate indicator, 4-(2-pyridylazo)resorcinol (PAR) was selected. PAR forms both 1:1 and 2:1 complexes with Zn^{2+}, with stepwise apparent affinity constants of 4.0×10^6 and 5.5×10^5 M^{-1}, respectively (at pH 7.0, $\mu = 0.1$).[47] Addition of Zn^{2+} to a solution of PAR produces an intense absorbance at 500 nm ($\Delta\epsilon = 6.6 \times 10^4$ M^{-1} cm^{-1}) which has been used for the
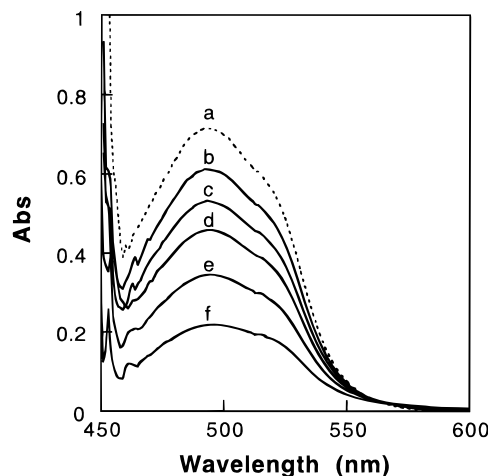
determination of low picomolar protein–zinc dissociation constants.[48] An excess of PAR, sufficient to assure $\geq 99\%$ of the Zn^{2+} bound to PAR was in the 2:1 form, was used. The results from a typical competition experiment are shown in Figure 7. Incremental additions of FS03DNS to a solution containing PAR and Zn^{2+} result in a decrease in the fraction of PAR involved in the PAR$_2$Zn complex, resulting in a diminution of the PAR$_2$Zn signal observed at 500 nm. The apparent dissociation constant for the FS03DNS·Zn^{2+} complex was determined to be 140 ± 30 pM.

FS04DNS. In light of the success of FS03DNS as a fluorescent sensor of divalent zinc, modification of the peptidyl template was undertaken to enhance the oxidative stability of the chemosensor. The naturally occurring metal binding residues, histidine, aspartic acid, and glutamic acid, were considered to replace one of the cysteines. Molecular modeling suggested that Cys^6 would be more tolerant toward residue substitution. Ultimately the change of Cys$^6 \rightarrow$ Asp was made to maintain the charge neutralization that is provided by the native thiolate ligand, and match the size of the replacement residue as closely as possible to that of the native ligand.

Modification of the ligand sphere of the zinc finger has little effect upon the extent of metal-induced structural change (Figure 6, dotted lines). The fluorescence properties of FS04DNS retain the Zn^{2+} sensitivity observed for FS03DNS. More importantly, FS04DNS is compatible with redox active metal cations such as Cu^{2+}. The fluorescence emission response of FS04DNS to divalent zinc is summarized in Table 3.

The Zn^{2+} binding affinity of the peptide FS04DNS was evaluated by a competition assay with mag-fura-2. Analysis revealed that treatment of the binding competition assuming 1:1 peptide–metal complex formation (as described for FS02DNS) did not suitably model the data. Initial formation of 2:1 peptide·Zn^{2+} complexes has been observed for other zinc finger peptides,[49,50] including a zinc finger-derived fluorosensor.[28] In those systems, Cys$_4$·Zn^{2+} complexes are formed at low Zn^{2+} concentrations due to the preference of the zinc ion for a soft ligand.[20,51] It is presumed that the proposed CysHis$_2$Asp

(42) Kochoyan, M.; Keutmann, H. T.; Weiss, M. A. *Proc. Natl. Acad. Sci. U.S.A.* **1991**, *88,* 8455–8459.

(43) Hoffman, R. C.; Horvath, S. J.; Klevit, R. E. *Protein Sci.* **1993**, *2,* 951–965.

(44) Lee, M. S.; Gippert, G. P.; Soman, K. V.; Case, D. A.; Wright, P. E. *Science* **1989**, *245,* 635–637.

(45) Omichinski, J. G.; Clore, G. M.; Appella, E.; Sakaguchi, K.; Gronenborn, A. M. *Biochemistry* **1990**, *29,* 9324–9334.

(46) Weiss, M. A.; Keutmann, H. T. *Biochemistry* **1990**, *29,* 9808–9813.

(47) Hunt, J. B.; Neece, S. H.; Ginsburg, A. *Anal. Biochem.* **1985**, *146,* 150–157.

(48) Jefferson, J. R.; Hunt, J. B.; Ginsburg, A. *Anal. Biochem.* **1990**, *187,* 328–336.

(49) Michael, S. F.; Kilfoil, V. J.; Schmidt, M. H.; Amann, B. T.; Berg, J. M. *Proc. Natl. Acad. Sci. U.S.A.* **1992**, *89,* 4796–4800.

(50) Shi, Y. G.; Beger, R. D.; Berg, J. M. *Biophys. J.* **1993**, *64,* 749–753.

(51) Pearson, R. G. *Science* **1966**, *151,* 172–177.

coordination sphere of FS04DNS operates within the same manifold, preferring at low Zn^{2+} concentrations to bind thiolate ligands to divalent zinc in the place of *N* or *O* ligands.

To further probe the Zn^{2+} binding behavior of FS04DNS, the apparent dissociation constant for the FS04DNS·Zn^{2+} complex was calculated from each spectrum in the mag-fura-2 competition experiment by applying a mathematical treatment analogous to that described for the PAR competition assays used with the peptide FS03DNS. At low concentrations of free Zn^{2+} (<20 nM) the apparent dissociation constant of the FS04-DNS·Zn^{2+} complex is indeterminate by this method. However, at free Zn^{2+} concentrations greater than 20 nM, the 1:1 complex is the dominant peptide−metal species and the apparent dissociation constant of the FS04DNS·Zn^{2+} complex is obtained as 65 ($\pm$ 5) nM.

Discussion

The development of an oxidatively robust fluorescent peptidyl chemosensor for divalent zinc has been presented. Several synthetic zinc finger peptides have been characterized by a variety of techniques including CD, UV−vis, and fluorescence spectroscopy. For each of these peptides, the apparent dissociation constant of the peptide−zinc complex has been determined, and all bind divalent zinc with high affinity. A summary of the zinc binding affinities of these peptides is provided in Table 2. A summary of the fluorescence emission properties of the dansylated peptides is presented in Table 3. Furthermore, the peptides FS03DNS and FS04DNS are useful as sensors for divalent zinc having appreciable fluorescence response, with FS04DNS being an oxidatively robust fluorosensor.

Selection of the Peptidyl Template. A metal cation chemosensor requires two parts of equal importance, a metal binding moiety and a fluorescent signaling moiety. The central challenge for the production of new chemosensors for divalent metal cations remains one of selectivity. The avid and selective binding of Zn^{2+} exhibited by the zinc finger peptides was therefore exploited for the metal binding (sensing) event. The native zinc finger peptides, however, lack a spectroscopic handle of sufficient sensitivity to signal this metal-dependent change. In these peptides a structural change from predominantly random coil to folded domains occurs upon binding Zn^{2+} which serves to alter the microenvironment of specific residues from being solvent exposed to participating in a hydrophobic cluster. Thus, to transduce this metal binding event in a chemosensor, a fluorophore-bearing residue was incorporated in the place of the residues involved in the hydrophobic cluster of a zinc finger peptide.

Importance of Metal-Induced Secondary Structural Changes. The efficacy of this mechanism of microenvironment sensitive fluorescence for signal transduction depends on the magnitude of the change experienced by the fluorophore. It is therefore expected that a large change in secondary structure upon binding Zn^{2+} would be accompanied by a concomitant change in fluorescence. Interpretation of the CD data is subject to the caveat that the fluorophores used in this study could contribute to the spectra in a manner unlike native proteins. Specifically the negative ellipticity observed for FS03DNS·Zn^{2+} between 250 and 280 nm (Figure 6c) is a feature not commonly observed for zinc finger complexes, and may result from the dansyl chromophore. However, the CD spectra of all the peptide·Zn^{2+} complexes obtained bear resemblance to those of naturally occurring zinc finger domains, regardless of the incorporated fluorophore. These results suggest that the CD spectra are not dominated by specific fluorophore-related effects.
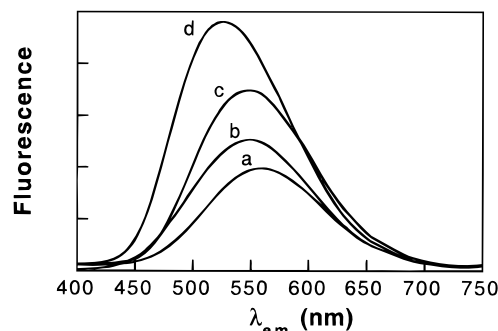

Figure 8. Fluorescence emission spectra of several peptide·Zn^{2+} complexes, corrected for the concentration of the fluorophore, as compared to the model compound dansyl asparagine: (a) dansyl asparagine, (b) FS02DNS·Zn^{2+}, (c) FS04DNS·Zn^{2+}, (d) FS03DNS·Zn^{2+}.

In any case, it is likely that a metal-dependent change in the CD spectrum for a given peptide is indicative of a concomitant change in the microenvironment of the fluorophore, whether it results solely from changes in secondary structural content or includes a contribution from the fluorophore itself.

This expectation is borne out by the CD studies performed on these peptides. Both FS01DMB and FS02DNS, which are derived from Zif268, show small changes in structure upon Zn^{2+} addition (Figure 2). By comparison, the Zn^{2+}-induced structural changes of FS03DNS and FS04DNS, which are derived from ZFY-swap, are much larger (Figure 6). Since FS02DNS, FS03DNS, and FS04DNS share the same fluorophore, the effect of structural change upon fluorescence may be compared directly with the caveat that the fluorophore is attached at a different position within the primary sequence of the former peptide. In these cases, larger metal-induced changes in secondary structure measured by CD correlate with larger changes in fluorescence emission. These results highlight the importance of the inherent structural content of the peptidyl template in the absence of metal cations for fluorescence signaling.

Accommodation of the Fluorophore within the Hydrophobic Cluster. Of paramount importance for the production of a sizable fluorescence response is the ability of the folded peptidyl template to accommodate the presence of a bulky fluorophore. For the dansyl chromophore, increasing emission intensity with increasing blue-shift indicates the fluorophore is in a less polar microenvironment. Thus, the protection of the fluorophore from bulk solvent provided by the peptidyl template may be estimated qualitatively from the emission spectra. Concentration-corrected fluorescence emission of spectra of the model compound dansyl asparagine and the zinc complexes of FS02DNS, FS03DNS, and FS04DNS are presented for comparison in Figure 8. The fluorescence emissions from the zinc complexes of FS03DNS and FS04DNS are the most blue-shifted and intense, indicating more complete accommodation of the dansyl group as a member of the hydrophobic cluster. However, the emission of the FS04DNS·Zn^{2+} complex is diminished considerably relative to that of FS03DNS·Zn^{2+}, which differs in only one residue. Clearly a subtle interplay exists between the geometry of the metal ligating residues and the topology of the folded peptide.

Ligand Choice and Zinc Binding Affinity. To construct an oxidatively robust sensor from the zinc finger template requires the substitution of one of the metal binding cysteines. However, substitution of the cysteine residues, which comprise the native metal coordination sphere, for other naturally occurring metal binding residues reduces the Zn^{2+} binding affinity exhibited by the template (Table 2). This is presumably due to the preference of ions with electronic configurations of d^{10} for

soft ligands.[52] Thus, the peptides FS01DMB and FS03DNS with S_2N_2 metal binding sites have the highest affinity for Zn^{2+}, followed by FS02DNS with a SN_3 site, and ultimately by FS04DNS which has an SN_2O ligation sphere.

Initial access to an oxidatively robust fluorescent chemosensor for divalent zinc was obtained in the peptide FS02DNS by making the substitution $Cys^6 \rightarrow His$ in the parent sequence of FS01DMB. While this peptide was tolerant of redox active metal ions, the fluorescence response to Zn^{2+} was too small to be useful as a sensitive probe of divalent zinc concentrations. In addition, fluorescence emission experiments carried out with competing Cu^{2+} and Zn^{2+} indicated that FS02DNS bound divalent copper with at least 2 orders of magnitude preference over zinc (data not sown). On the basis of this knowledge, alternate ligating residues were considered for incorporation in the place of cysteine for the design of FS04DNS. Aspartic acid was selected as a replacement for Cys^6 to most closely mimic the steric and charge neutralization properties of the thiolate ligand. In addition, the carboxylate ligand exhibits flexible coordination geometry,[53] which was expected to relax the stringent steric requirements for metal ligation.

Modification of the ligation sphere of FS03DNS resulted in the production of a fluorescent peptidyl chemosensor for divalent zinc with enhanced oxidative stability. The fluorescence response of FS04DNS is responsive to submicromolar to micromolar concentrations of Zn^{2+}, in the presence of redox active metal cations (Cu^{2+}, Fe^{2+}) and vast excesses of the competing divalent cations Mg^{2+} and Ca^{2+} (Table 3). It is particularly relevant that this chemosensor is compatible with a ≥ 50000-fold excess of Mg^{2+} and ≥ 10000-fold excess of Ca^{2+} given the concentration of these species in biological samples.

Conclusion

The zinc finger motif provides an architecture which is viable for the production of fluorescent sensors. The ease with which the peptide scaffold may be modulated provides opportunity for the continued elaboration of this design. The affinity of the zinc finger motif for divalent zinc may be varied by the choice of chelating residues as well as the overall amino acid sequence. Through the modification of ligand type, a fluorescent chemosensor for divalent zinc with enhanced oxidative stability has been produced. Future modifications to this design may include the peptide incorporation of nonnatural, bidentate chelating residues to augment the metal binding selectivity of the motif as well as the incorporation of ligands with metal-modulated fluorescence properties.

Experimental Section

Peptide Synthesis. Peptides were synthesized on a Milligen 9050 peptide synthesizer on a 0.125 mmol scale. Fmoc-PAL-PEG-PS (PerSeptive) resin (0.21 mmol/g) was used to afford carboxy-terminal primary amides. Couplings were performed at a concentration of 0.3 M acylating reagent and 1-hydroxybenzotriazole (HOBt), in a volume sufficient to achieve a 3-fold excess of amino acid to resin-bound amine. Pentafluorophenyl ester/HOBt chemistry was employed for all residues except Fmoc-L-Baa(alloc)-OH which was coupled by *in situ* active ester generation using HOBt/*N,N*′-diisopropylcarbodiimide activation. A double-coupling procedure was employed, with coupling reactions of 45 min, followed by a 10 min wash with 0.3 M acetic anhydride/HOBt solution in 9:1 DMF/dichloromethane to cap any unreacted amines. Removal of the Fmoc group was performed with piperidine (20% v/v in DMF) with a standard wash duration of 7 min. After addition of the final residue, the amino terminus was acetyl-capped (DMF/acetic

Table 4. Calculated and Observed Electrospray Mass Values for the Synthetic Zinc Finger Peptides

peptide	formula	$[MH^+]_{calcd}$	$[MH^+]_{obsd}$
FS01DMB	$C_{120}H_{188}O_{40}N_{37}S$	2853.2	2852.6
FS02DNS	$C_{126}H_{192}O_{42}N_{39}S_2$	2973.3	2973.5
FS02CMN	$C_{124}H_{185}O_{42}N_{41}S$	2912.2	2912.6
FS03DNS	$C_{138}H_{214}O_{42}N_{42}S_3$	3230.7	3231.0
FS04DNS	$C_{139}H_{215}O_{44}N_{42}S_2$	3240.5	3241.3

anhydride/triethylamine, 4 mL:63 μL:94 μL) for 0.5 h and then washed with DMF (5 × 10 mL) and MeOH (5 × 10 mL). Residual solvent was removed under reduced pressure.

Allyloxycarbonyl Removal. The method of Kates et al.[30] was employed with some minor modifications. A typical procedure for removal of the allyloxycarbonyl (alloc) group was as follows. Under a blanket of nitrogen, a 20-mL plastic, stoppered vial was charged with resin from the completed peptide synthesis (300 mg, 0.21 mequiv/g, 63 μmol), and 5 mL of a solvent cocktail (CHCl$_3$/morpholine/AcOH, 90:5:5). The resin was allowed to swell for 10 min, and then tetrakis-(triphenylphosphine)palladium (200 mg, 173 μmol) was added under a blanket of nitrogen. The vial was capped, shielded from light, and placed on a wrist-action shaker at low speed for 2 h. The resin was filtered and washed with CHCl$_3$ (5 × 10 mL) and a palladium chelating cocktail (DMF/diethyldithiocarbamic acid·3H$_2$O / triethylamine, 25 mL: 225 mg:250 μL). Traces of this solution were removed with a basic wash (0.5% v/v triethylamine in DMF), and a final wash with methanol. The resin was transferred to a clean plastic vial, and the residual solvent removed under reduced pressure.

Fluorophore Coupling. Lyophilized resin was taken directly from the alloc-removal procedure, and allowed to swell in DMF (5 mL). For addition of the dansyl group, 10 equiv (based on resin-bound amine) of dansyl chloride was added, followed by 10 equiv of triethylamine. Coupling of 4-(dimethylamino)benzoic acid or 3-carboxycoumarin was performed with standard ((benzotriazol-1-yloxy)tris(dimethylamino)-phosphonium hexafluorophosphate (BOP) coupling. In all cases, after the addition of the acylating reagent, the vial was capped under a blanket of nitrogen, and placed on a wrist-action shaker at low speed for 2 h. The resin was filtered, washed with a basic wash (5 × 10 mL, see above), washed with DMF (5 × 10 mL), then finally washed with MeOH (5 × 10 mL). The resin was transferred to a clean 20-mL polyethylene vial, and residual solvent was removed under reduced pressure prior to peptide cleavage.

Peptide Cleavage and Purification. Peptides were cleaved after fluorophore coupling using 10 mL of Reagent K[54] (trifluoroacetic acid/ H$_2$O/ethanedithiol/thioanisole/phenol, 82.5:5:5:5:2.5) with a 2-h incubation period. The resin was filtered, concentrated to ca. 2-mL volume, and precipitated with ether/hexane (2:1) at -20 °C for 30 min. The supernatant was decanted, and the solid triturated with ether/hexane (2:1) (5 × 50 mL). The resultant solid was resuspended in water (20 mL), lyophilized, and then purified to homogeneity by reversed phase (C$_{18}$) high-performance liquid chromatography (HPLC). The identity of each peptide was confirmed by electrospray mass spectroscopy (Table 4).

Peptide Stock Solutions. After HPLC purification, the fractions containing pure peptide were lyophilized, and resuspended in hydrogen-sparged water to retard oxidation. When not in use, stocks were stored at -80 °C. The concentration of the stock solutions was determined by reaction with Ellman's reagent, 5,5′-dithiobis(2-nitrobenzoic acid) (DTNB).[55] These assays were performed in triplicate, with excellent agreement (<5% variance) between runs. From the concentration of the stock solution, the extinction coefficient of the peptide was determined at a wavelength appropriate for the fluorophore present. All peptide concentrations were determined subsequently on the basis of this value. As the reduced and oxidized (disulfide) forms of the peptides are separable by HPLC, aliquots of the stock solution were periodically checked to assure that no detectable oxidation had occurred.

(52) Cotton, F. A.; Wilkinson, G. *Advanced Inorganic Chemistry*; John Wiley & Sons, Inc.: New York, 1988.

(53) Glusker, J. P. *Adv. Protein Chem.* **1991**, *42*, 1−76.

(54) King, D. S.; Fields, C. G.; Fields, G. B. *Int. J. Pept. Protein Res.* **1990**, *36*, 255−266.

(55) Riddles, P. W.; Blakeley, R. L.; Zerner, B. *Methods Enzymol.* **1983**, *91*, 49−60.

Metal Stock Solutions. Stock solutions of divalent metal cations were prepared from analytical grade salts, and dissolved in high-purity water obtained from a Milli-Q (Millipore) filtration apparatus. The concentration of each stock solution was determined by titration against a standardized solution of EDTA (Aldrich) in the presence of an appropriate metallochromic indicator.[56]

Buffer Preparation. All buffers were prepared in acid-washed polyethylene containers using high-purity water obtained from a Milli-Q filtration apparatus. Sodium chloride and 4-(2-hydroxyethyl)-1-piperazineethanesulfonic acid (HEPES) were obtained from Sigma and used without further purification. After preparation of the buffer, the solution was passed through a 30 cm × 1.5 cm column of freshly regenerated Chelex resin (sodium form, Bio-Rad Laboratories).[57] This buffer was tested for metal ion impurities by the addition of 100 μM 4-(2-pyridylazo)resorcinol (PAR) followed by the addition of 1 mM EDTA, pH 7.0. The absorbance change at 500 nm in a 1.0-cm cell upon the addition of EDTA was ≤0.003, indicating that ≤50 nM divalent metal was present (assuming all metal ion impurities were Zn^{2+}, $\Delta\epsilon_{500} = 6.6 \times 10^4$). This buffer test was performed periodically to test against buffer contamination.

Circular Dichroism. Spectra were recorded on a Jasco J600 circular dichroism spectrometer. The peptide concentration in each assay was determined spectrophotometrically on a Shimadzu UV-160 UV−vis spectrophotometer fitted with a circular cell holder. Except for pH dependence studies, which were performed in unbuffered water, spectra were acquired in 0.5 mM HEPES, pH 7.0. In general, a nominal concentration of 10 μM peptide was used in a 1.0-cm cell. Spectra were baseline corrected and noise reduced using the Jasco software.

Emission Fluorescence Assay. Assays were performed with a SLM-Aminco SPF-500c spectrofluorometer at room temperature in 50 mM HEPES buffer, pH 7.0, 0.5 M NaCl, in a stoppered 750 μL (1 cm × 3 mm) quartz fluorometer cell. The concentration of peptide in a given assay was determined by absorption spectroscopy immediately prior to the fluorescence experiment. Emission spectra were accumulated at 1-nm intervals with the following parameters: excitation band pass 4 nm, emission band pass 2 nm, lamp potential 975 V, gain 10, filter (time constant) 3.

Competitive Zinc Binding with 4-(2-Pyridylazo)resorcinol (PAR). A method for the determination of subpicomolar protein−zinc dissociation constants has been described previously,[47] and a modified version of this procedure was employed. Because PAR forms both 1:1 and 2:1 complexes with Zn^{2+}, an excess of PAR must be used that is sufficient to put ≥99% of the zinc bound to PAR in the 2:1 PAR·Zn^{2+} form. Thus, the binding equilibrium may be expressed as in eq 1. Under these conditions, the apparent affinity constant of the peptide may be obtained by solving eq 2 for K'_{Pep}.

$$Pep + PAR_2Zn = Zn \cdot Pep + 2PAR \qquad (1)$$

$$\frac{[Zn \cdot Pep][PAR]^2}{[Pep][PAR_2Zn]} = \frac{K'_{Pep}}{\beta'_{PAR}} \qquad (2)$$

The dissociation constant of the Zn·Pep complex was calculated by substituting into eq 2. Equations 3−6 were used to calculate the individual components of eq 2. Competition experiments were performed with nominal PAR concentrations of 200, 240, and 300 μM to assure that the zinc binding competition is adequately represented by eq 1.

$$[PAR_2Zn] = \frac{A_{500}}{\Delta\epsilon_{500}} \quad \text{where} \quad \Delta\epsilon_{500} = 6.6 \times 10^4 \qquad (3)$$

$$[PAR] = [PAR]_{total} - 2[PAR_2Zn] \qquad (4)$$

$$[Zn \cdot Pep] = [PAR_2Zn]_{initial} - [PAR_2Zn] \qquad (5)$$

$$[Pep] = [Pep]_{total} - [Zn \cdot Pep] \qquad (6)$$

Competition Assay with PAR. Assays were performed on a Beckman DU-700 UV−vis spectrophotometer at room temperature

using a standard 1.0-cm-path-length cell. Repeat runs were performed at a variety of PAR concentrations to assure that a simple zinc binding competition was in effect. A typical assay is described. Aliquots of HEPES buffer (979 μL) and the PAR stock solution (21 μL) were mixed in a cuvette, and the spectrophotometer was blanked against this solution. A 1.9-μL aliquot of 5.30 mM Zn^{2+} was added, and the UV−vis spectrum was acquired between 200 and 700 nm. The increased absorbance at 500 nm results from the formation of the PAR$_2$Zn complex which has a $\Delta\epsilon = (6.6 \pm 0.2) \times 10^4 \, M^{-1} \, cm^{-1}$, corrected for pH.[47] Aliquots of a 1.75 mM stock solution of FS03DNS were added in 2.0-μL increments, and the absorption spectrum was recorded.

PAR Stock Solution. The monosodium salt hydrate of 4-(2-pyridylazo)resorcinol was obtained from Aldrich, and dried under reduced pressure over P_2O_5 for two days at 50 °C. A 9.62 mM solution of PAR was then prepared by dissolving 22.8 mg of the freshly dried material in 10.0 mL of water. After dissolution, this stock solution was stored in the dark at 4 °C.

Competitive Zinc Binding with Mag-fura-2. The apparent dissociation constant of the mag-fura-2·Zn^{2+} complex is 20 nM at pH 7.0 and ionic strength 0.15.[41] Consequently, assays performed with mag-fura-2 were conducted in 50 mM HEPES buffer, pH 7.0, $\mu = 0.15$ (NaCl), which was treated to remove adventitious divalent metal ions, and tested for impurities as described above. An aliquot of peptide stock solution (sufficient to deliver 15−30 nmol of peptide) was added to a 1.0-cm cuvette followed by buffer to bring the volume up to 960 μL. The spectrophotometer was blanked against this solution, and then 9.0 μL of the stock mag-fura-2 solution was added. The concentration of the mag-fura-2 actually delivered was calculated from the absorbance at 366 nm ($\epsilon(366) = 29\,900 \, M^{-1} \, cm^{-1}$). Small aliquots of a standardized 1.00 mM solution of $ZnCl_2$ (2.0−4.0 μL) were added, with spectra taken between additions.

Dissociation constants were extracted using literature methods.[40] The variables Q and P are solved using eqs 7 and 8, respectively. Q is

$$Q = \frac{\epsilon - \epsilon_{IL}}{\epsilon_I - \epsilon} \qquad (7)$$

$$P = L_t - 1/QK_I - I_t/(Q + 1) \qquad (8)$$

equal to the ratio of free indicator to metal-bound indicator, ϵ, ϵ_I, and ϵ_{IL} are the observed, free, and metal-bound indicator extinction coefficients, respectively. P is the concentration of peptide−metal complex, L_t is the total ligand (metal) concentration, K_I is the association constant for the indicator−metal complex, and I_t is the total indicator concentration.

It can be shown that these variables are related as in eq 9. Thus, the binding affinity of the peptide is determined by plotting S_t/P as a function of Q, where S_t is the total substrate (peptide) concentration, and K_{Pep} is the association constant of interest.

$$\frac{S_t}{P} = (K_I/K_{Pep})Q + 1 \qquad (9)$$

Supporting Information Available: UV−vis absorption spectra and data reduction for the Zn^{2+} binding analysis of FS04DNS (5 pages). See any current masthead page for ordering and Internet access instructions.

JA9642121

(56) *Vogel's Textbook of Quantitative Inorganic Analysis*; Bassett, J., Denney, R. C., Jeffery, G. H., Mendham, J., Eds.; William Clowes: London, 1978; pp 223−402 .

(57) Holmquist, B. *Methods Enzymol.* **1988**, *158*, 6−12.